Wang, Y., Huang, T., Jin, S., Wang, C., Shen, H., Li, C., Li, Y. and Wu, W. (2022) A self-biased GaN LNA with 30 dB Gain and 21 dBm P1dB for 5G communications. *International Journal of Microwave and Wireless Technologies*, 15(4), pp. 547-553.(doi: 10.1017/S175907872200085X).

This is the Author Accepted Manuscript.

There may be differences between this version and the published version. You are advised to consult the publisher's version if you wish to cite from it.

http://eprints.gla.ac.uk/273673/

Deposited on: 24 June 2022

Enlighten – Research publications by members of the University of Glasgow
http://eprints.gla.ac.uk

A Self-biased GaN LNA with 30 dB Gain and 21 dBm P_{1dB} for 5G Communications

Yi Wang [1], Tongde Huang [1], Saisai Jin [2], Chong Wang[2], Hongchang Shen[2], Chong Li[3], Yuehua Li[1], Wen Wu[1]

[1] Ministerial Key Laboratory of JGMT, Nanjing University of Science and Technology, Nanjing, 210094, China.

[2] Nanjing Guobo Electronics Co., Ltd, Nanjing, 210000, China.

[3] James Watt School of Engineering, University of Glasgow, Glasgow, G12 8LT, U.K.

We present a self-biased three-stage GaN-based Monolithic Microwave Integrated Circuit (MMIC) Low-noise Amplifier (LNA) operating between 26 GHz and 29 GHz for 5G mobile communications. The self-biasing circuit, common-source topology with inductive source feedback, and RLC negative feedback loops between gate and drain of the third transistor were implemented to achieve low noise, good port match, high stability, high gain and compact size. Measurement results show that the LNA has a high and flat gain of 30.5±0.4 dB with NF of 1.65-1.8 dB across the band. The three-stage topology also achieves high linearity, providing the 1-dB compression point output power (P_{1dB}) of 21 dBm in the band. To our knowledge, this combination of NF, gain and linearity performance represents the state of art of self-biased LNA in this frequency band.

Corresponding author: Tongde Huang; email: tongdeh@njust.edu.cn

I. INTRODUCTION

The first 5th generation (5G) mobile network was rolled out in South Korea in 2019. Comparing the previous generations, 5G provides much higher capacity and lower latency to tackle the problem caused by the ever-increasing data, number of connected devices and emerging applications. To achieve this, wider bandwidth and more frequency bands have been assigned to 5G including sub-6 GHz bands and millimeter-wave (mmWave) bands such as 26 - 30 GHz [1],

[2]. Although mmWave can provide a chunk of continuous bandwidth up to GHz, only a few countries have adopted it in reality; most deployed 5G networks are running at sub-6 GHz bands. One of the major challenges for not deploying mm-wave 5G lies in the immature technology for frontends, causing low gain, low power efficiency and high cost. Low noise amplifiers (LNAs) are critical components in the frontend of all communication systems usually located at the first stage of the receiver after the antenna. Typical semiconductor technologies for LNAs are divided into two categories: silicon and III-V. The former includes CMOS, SiGe BiCMOS, and silicon on insulator (SOI) and has the advantages of low power consumption, high integrability, low cost and compact size but poor in noise figure and gain [3], [4]. The latter consists of conventional InP [5] and GaAs [6] high mobility transistors (HEMTs) which have lower noise figure (NF) and higher gain than the silicon technologies. More recently, GaN HEMT has received great attention for its excellent performance in both low noise and high power [7] - [9]. Compared with GaAs and InP, one of the significant advantages of GaN LNAs is their high-power handling capability which is preferable in complex electromagnetic environments e.g. remote sensing in space or satellite communications where additional measures e.g. limiters must be implemented to protect the receivers. In addition, the high-power tolerance ability is also desirable in signal detection and electronic countermeasure (ECM) and Multiple Input Multiple Output (MIMO) communications [7].

In this work, we demonstrate a three-stage monolithic integrated GaN LNA operating between 26 GHz and 29 GHz for mmWave 5G applications. Unlike reported GaN LNAs elsewhere [10], [11], the LNA demonstrated here has three stages but is powered by a single power supply. Such a design simplifies biasing circuits and makes the whole circuit more compact. The measured gain and P_{1dB} are around 30.5±0.4 dB and 21 dBm, respectively. The NF is 1.65-1.8 dB in 26 - 29 GHz. The measured S_{11} and S_{22} are both below -10 dB across the whole band. The results show the proposed GaN LNA could be ideal candidates for mm-wave 5G.

II. LNA DESIGN

A) The HEMT and Its Small-signal Modal

The GaN transistor used in this work is 2×30 μm and is developed using a 0.1 μm depletion mode. Fig. 1 shows its small signal equivalent circuit. The initial bias conditions of the device were chosen to achieve the maximum value of $f_T \times g_m / I_{DS}$, where f_T, g_m, and I_{DS} are transition frequency, transconductance, and source-drain current, respectively [12-15]. However, the ultimate optimal bias voltages at the gate and drain i.e. V_g = -2 V and V_d = 15 V, respectively, are decided as a compromise among matching loss, NF, gain and stability. In order to match the input impedance (Z_{in}) of the LNA to 50 Ω, an inductive degeneration was adopted, making the real part of Z_{in} equal to $2\pi L_{seff} + R_s$, where the L_{seff} is the effective source or emitter inductance and R_s is the source resistance. The measured S-parameters of the transistor are shown in Fig. 2 and extracted values of the small-signal equivalent circuits are shown in Table 1. The simulated results based on the model are in good agreement with the measured ones.

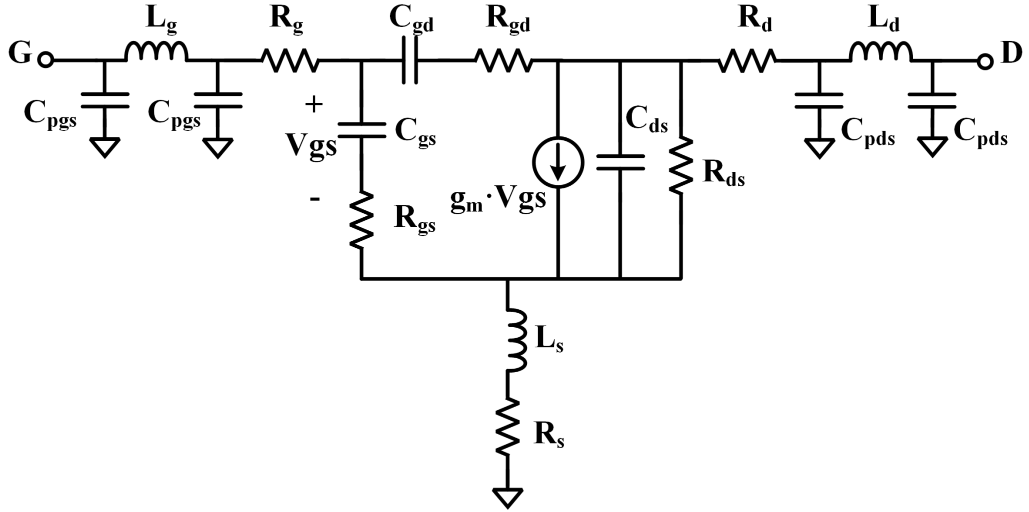

Fig. 1. Small-signal circuit model of GaN HEMT at the bias point of V_g = -2 V and V_d = 15 V.

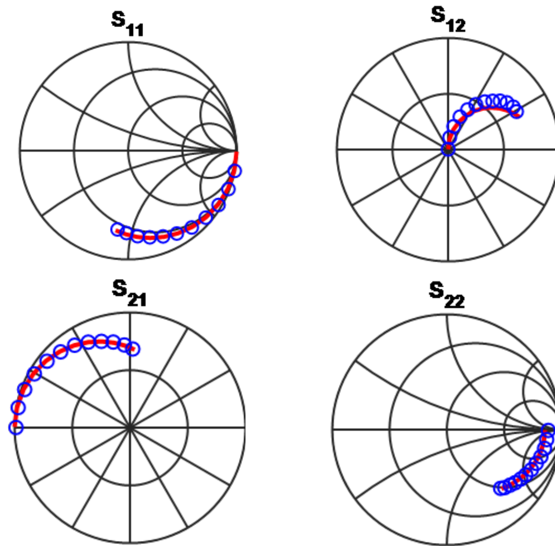

Fig. 2. The measured (blue circle) and modelled (red line) S-parameters.

The frequency range is from 0.2 to 60 GHz.

Table 1. Extracted intrinsic small-signal parameters of the GaN HEMTs.

Intrinsic parameters	g_m (mS)	R_{ds} (Ω)	R_s (Ω)	R_d (Ω)	L_s (pH)	C_{gs} (fF)	C_{gd} (fF)
Value	84.5	192	22.9	64.9	5.8	47.9	5.1

B) LNA Design

In this work, we used a common source cascaded 3-stage architecture to achieve a minimum gain of 30 dB, which is higher than the state of art LNAs operating at the same frequency range, while keeping NF as low as possible as shown in Fig. 3. The overall NF in a cascaded system is determined by the well-known Friis equation

$$NF = NF_1 + \frac{NF_2 - 1}{G_1} + \frac{NF_3 - 1}{G_1 G_2} \cdots \tag{1}$$

where NF_x and G_x (x = 1, 2, 3) are NF and gain of the xth stage of the cascaded LNA in a linear scale. The gain and NF of the first stage are more important than those of the following stages. Since HEMTs are constructed in a common source topology and the same HEMTs are used for all stages, the main task is then focused on input matching for minimizing the NF and lowering the input return loss at the first stage. The final stage serves the purpose of maximizing gain, improving the flatness of the gain, and reducing output return loss. A series *RLC* negative feedback loop is applied between the gate and drain of the third stage to adjust the gain flatness and improve the stability. However, its contribution to the overall NF is very limited as seen in (1). The inter-stage is tuned to ensure noise, gain, and input and output standing wave ratio meet the overall goal. A feedback inductor was deployed at the source of HEMT to achieve minimum NF and low input return loss simultaneously, which is challenging in many cases, by rotating S_{11} of the LNA close to the optimum reflection coefficient Γ_{opt} for noise at the first stage [10] and achieve both optimal noise matching and input conjugate matching [19]. Finally, the inductive source feedback can also improve the stability. Although the inductive degeneration does not have the same impact on the NF as resistive degeneration does, it still reduces the overall gain of the circuit.

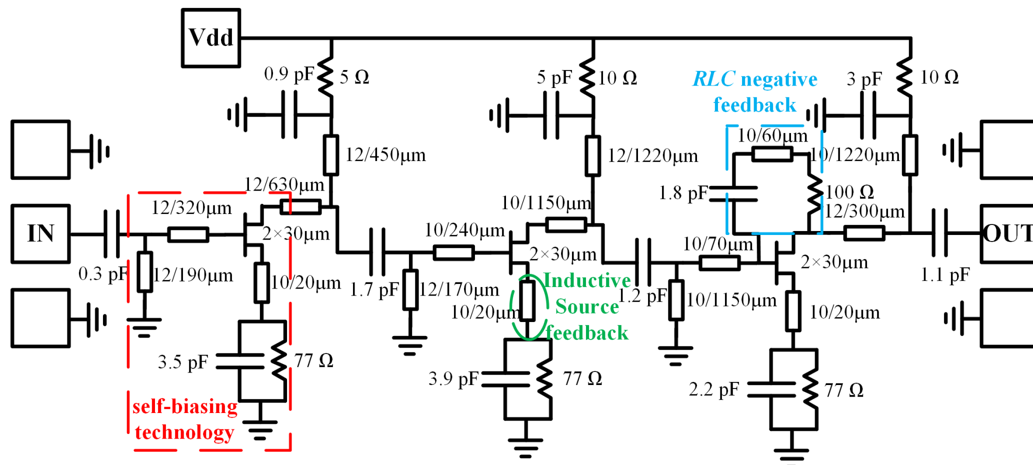

Fig. 3. Simplified schematic of the designed LNA.

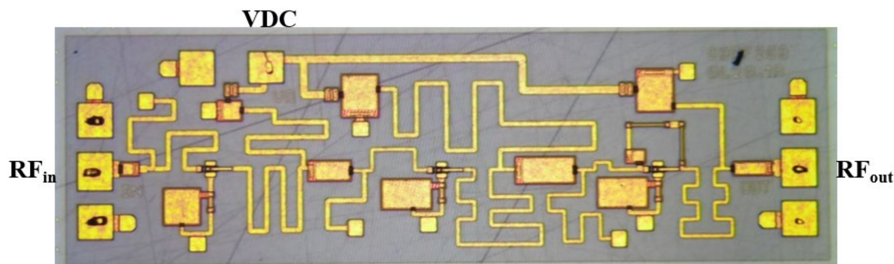

Fig. 4. Photograph of the fabricated LNA.

C) Biasing Circuit

A self-biasing technology is utilized to power all HEMTs conveniently through a single drain voltage, providing greater flexibility of biasing conditions [17], [18]. As shown in Fig. 3, the circuit contains a shunt resistor (R) and capacitor. The capacitor acts as a bypassing capacitor, helping to filter the noise contribution from the feedback resistor and improve the gain at the interested frequency range. The negative voltage on the resistor (R) is supplied to the gate through the grounded microstrip of the input matching circuit that, as part of source impedance matching, simplifies the input matching network, thus the V_g can be expressed as $-I_{DS}\cdot R$. In the proposed LNA, the value of I_{DS} and R is 25.9 mA and 77 Ω which make the HEMT is biased at V_g = -2 V and V_d = 15 V. Although careful design and several iterations of process validation have been made, the process variation may still cause effect on the self-biasing circuit. In fact, we implemented a laser trimming on the resistor for fine-tuning. It should be noted that, due to the presence of the capacitor, much more care should be taken in stability simulation. A quarter-wavelength stab with a resonant capacitor and a resistor in the drain bias line is used as an RF choke for stability improvement in each stage. Besides, the whole circuit has only two bonding pads in the drain, which can largely ease the bonding and packaging work. The overall bias circuits are more favourable for practical applications.

III. MMEASUREMENTS AND DISCUSSION

Fig. 4 shows the fabricated MMIC LNA that has an area of 0.8×2.4 mm^2. Although -2 V and 15 V are required for gate and drain of the HEMT, respectively, only 15 V was needed because a self-basing technology was adopted. S-parameter measurements were made on chip with ground-signal-ground probes at room temperature and the results are shown in Fig. 5 and Fig. 6. As can be seen, the measured S_{11} and S_{22} are below -10 dB between 26 GHz and 29 GHz, indicating that both the input and output matching are good. Moreover, the measured gain is 30.5±0.4 dB in the same frequency range. The simulated results are also plotted against the experimental results, and good agreements have been achieved. The cold source method was used to measure NF and both the experimental and simulated results are shown in Fig. 6 (b). One can notice that the measured NF is between 1.65 dB and 1.8 dB in the band, and the discrepancy

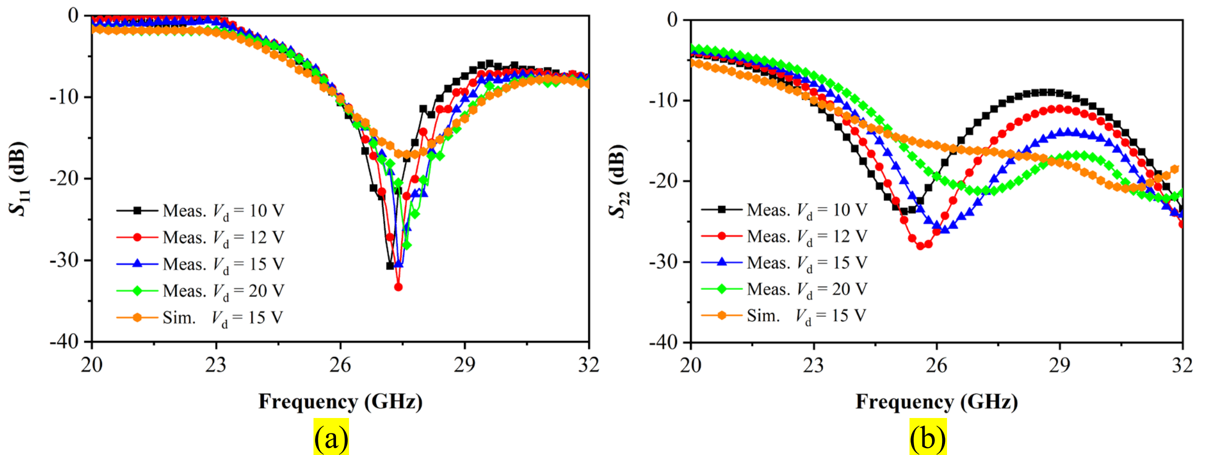

Fig. 5. Measured and simulated S_{11} (a) and S_{22} (b) at different bias points.

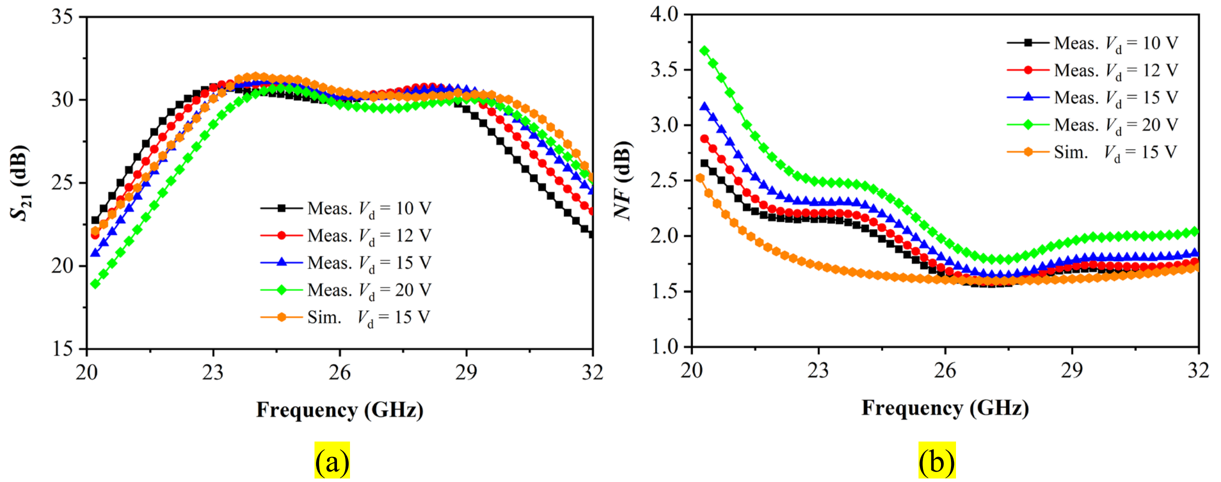

Fig. 6. Measured and simulated S_{21} (a) and NF (b) at different bias points.

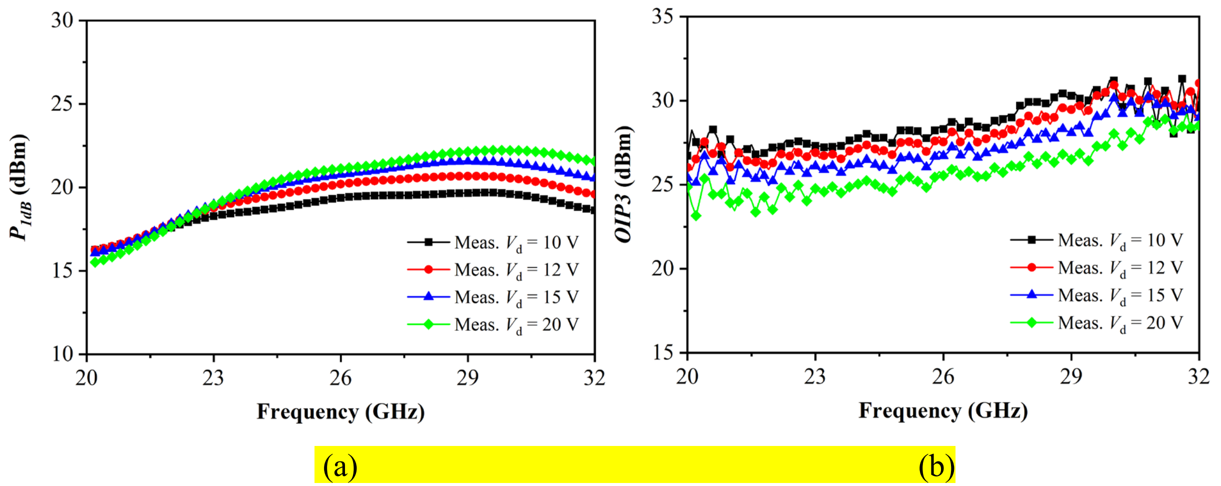

Fig. 7. Measured P_{1dB} (a) and $OIP3$ (b) of different bias points.

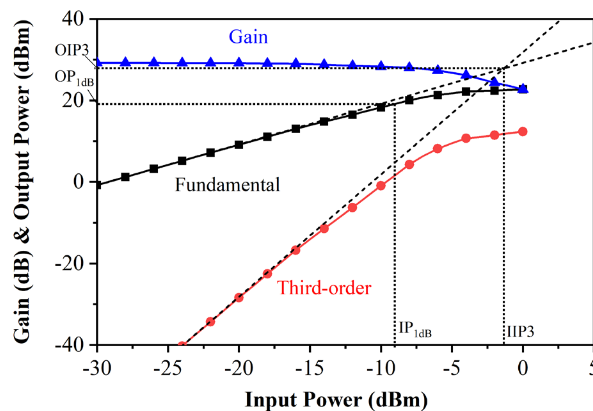

Fig. 8. Measured gain and output power versus input power at 28 GHz (biased at V_d=15 V, with RF and DC pads bonded to board).

between the measurement and simulation is smaller than 0.3 dB. The linearity of the LNA was also investigated and the results are shown in Fig. 7. The measured P_{1dB} and $OIP3$ are around 21 dBm and 27 dBm, which are much higher than that of GaAs and InP LNAs. Fig. 8 shows the

Table 2. Comparisons of LNAs for mmWave 5G using different semiconductor technologies.

Ref.	Tech.	Freq. (GHz)	Gain (dB)	NF (dB)	P_{1dB} (dBm)	Size (mm^2)	P_{DC} (mW)
[5]	0.1 μm InP	26-40	21-22.8	1.3-1.9	NA	2.1×0.82	14
[11]	0.15 μm GaN	27-31	15-20	3.7-3.9	NA	1.2×3.4	280
[6]	0.15 μm GaAs	25-40	18.7-21.7	2.2-2.8	NA	2.5×1.2	230
[19]	65 nm CMOS	25-30	17-21	>3.7	NA	0.2×0.85	10
[20]	130 nm CMOS	26.3-28	17-20	5.2-7.5	NA	0.27	24
[4]	22 nm FD-SOI CMOS	26.6-31.6	16-19.3	4.8-5.2	-18	0.705×0.38	11.4
[10]	0.1 μm GaN	23-31	22-27.5	0.93-1.4	22-25	1.9×0.8	NA
This work	0.1 μm GaN	26-29	30.1-30.9	1.65-1.8	21	2.4×0.8	1165

measured gain and output power versus input power at 28 GHz when the LNA is biased at V_d = 15 V. Note the measured *OIP3* and the results in Fig. 8 were obtained after the chip was packaged, which are slightly lower than the results under on-chip measurement due to the influence of wire bonding and package.

The analysis of the fabricated LNA is also performed at different bias points (10-20 V) as shown above. It is observed that the device performs better in terms of return losses and gain at lower bias drain voltages. Nevertheless, the gain ripple remains to be the same for all the cases. The designed LNA gives promising results to all four bias conditions. It is noticed that the LNA can accommodate a wide range of supply voltages from 10 - 20 V, which is preferred in radar system in practice.

To comprehensively compare the performance of the designed LNA, several performances of the recently published LNAs using different semiconductor techniques for mmWave 5G along with the LNA in this work are summarized in Table 2. We can observe that the noise of our work is obviously lower than the works based on CMOS technique. Moreover, it is conspicuous that the single power supply employed in this work can ensure a competitively excellent performance compared with other works powered by dual sources using the same technique. It is known that the main drawback of the self-biasing technique is sacrificed gain and noise figure. In addition, this LNA has a relatively high and flat gain as well as a high P_{1dB} of 21 dBm compared to GaAs and InP LNAs. Meanwhile, the high linearity sacrifices the power consumption, which is much higher than LNAs using other technologies. The measured NF is slightly higher than that of other LNAs based on 0.1 μm GaN process, which is caused by the resistor in the adopted self-biasing circuits. However, the adopted self-biasing structure simplifies the external circuitry.

IV. CONCLUSION

A GaN LNA based on 0.1-μm GaN MMIC process operating at 26 to 29 GHz is demonstrated in this work. The single power supplied LNA has a high and flat gain of 30.1-30.9 dB along with good input and output matching. The NF is about 1.65-1.8 dB in the band. The LNA has good linearity with P_{1dB} around 21 dBm. Compared with the published LNAs, the LNA in this work exhibits a competitive NF and a relatively high and flat gain as well as high linearity. In addition, this single power-supplied LNA provides ease of use and simplifies the overall system on account of the powering method compared to that of the two power-supplied LNA. To our

knowledge, the combination of NF, gain, and linearity performance represents the state of art of self-biased LNAs which is suitable for 5G communications.

ACKNOWLEDGEMENT

This work was supported in part by the National Natural Science Foundation of China (NSFC) under Grant 61804077, and in part by the Jiangsu Science and Technology Department under Grant BE2019116.

REFERENCES

[1] El-Halwagy W, Nag A, Hisayasu P, Aryanfar F, Mousavi P, Hossain M.: A 28-GHz quadrature fractional-N frequency synthesizer for 5G transceivers with less than 100-fs jitter based on cascaded PLL architecture. IEEE Trans Microwave Theory Tech. (2017), 65(2): 396–413.

[2] Azim R, Meaze AKMMH, Affandi A, Alam MM, Aktar R, Mia MS, Alam T, Samsuzzaman M, Islam MT. A multi-slotted antenna for LTE/5G Sub-6 GHz wireless communication applications. International Journal of Microwave and Wireless Technologies, (2021)13, 486–496.

[3] Mendes L, Vaz J C, Passos F, et al.: In-Depth Design Space Exploration of 26.5-to-29.5-GHz 65-nm CMOS Low-Noise Amplifiers for Low-Footprint-and-Power 5G Communications Using One-and-Two-Step Design Optimization. IEEE Access, (2021), 9: 70353-70368.

[4] Xu X, Schumann S, Ferschischi A, et al.: A 28 GHz and 38 GHz High-Gain Dual-Band LNA for 5G Wireless Systems in 22 nm FD-SOI CMOS, 2020 15th European Microwave Integrated Circuits Conference (EuMIC). Netherlands, 2021: 77-80.

[5] Tang Y L, Wadefalk N, Morgan M A, et al.: Full Ka-band high performance InP MMIC LNA module, 2006 IEEE MTT-S International Microwave Symposium Digest. San Francisco, CA, 2006: 81-84.

[6] Wang G, Chen W, Liu J, et al.: Design of a broadband Ka-band MMIC LNA using deep negative feedback loop. IEICE Electronics Express, (2018), 15(10): 20180317-20180317.

[7] X. Tong, L. Zhang, P. Zheng, S. Zhang, J. Xu and R. Wang: An 18–56-GHz Wideband GaN Low-Noise Amplifier with 2.2–4.4-dB Noise Figure. IEEE Microwave and Wireless Components Letters, (2020), vol. 30, no. 12, pp. 1153-1156.

[8] Rautschke F, May S, Drews S, Maassen D, Boeck G.: Octave bandwidth S- and C-band GaN-HEMT power amplifiers for future 5G communication. International Journal of Microwave and Wireless Technologies (2018),10, 737–743.

[9] O. K. W. Kobayashi, D. Denninghoff and D. Miller.: A Novel 100 MHz–45 GHz Input-Termination-Less Distributed Amplifier Design with Low-Frequency Low-Noise and High Linearity Implemented with A 6 Inch 0.15 um GaN-SiC Wafer Process Technology. IEEE Journal of Solid-State Circuits, (2016), vol. 51, no. 9, pp. 2017-2026.

[10] Zheng P, Zhang S, Xu J, Wang R, Tong X.: A 23-31 GHz gallium nitride highrobustness low-noise amplifier with 1.1-dB noise figure and 28-dBm saturation output power. Microw Opt Technol Lett. (2020), 62:1077–1081.

[11] Rudolph M, Chaturvedi N, Hirche K, et al.: Highly rugged 30 GHz GaN low-noise amplifiers. IEEE Microwave and Wireless Components Letters. (2009), 19(4):251-253.

[12] 0. J. Schleeh.: Cryogenic ultra-low noise InP high electron mobility transistors. Chalmers University of Technology, Sweden, 2013.

[13] F. Thome, P. Brückner, S. Leone and R. Quay: A Wideband E/W-Band Low-Noise Amplifier MMIC in a 70-nm Gate-Length GaN HEMT Technology. IEEE Transactions on Microwave Theory and Techniques, (2022), vol. 70, no. 2, pp. 1367-1376.

[14] A.S.A. Fletcher, D. Nirmal, L. Arivazhagan, et al.: A 28-GHz Low-Loss AlGaN/GaN HEMT for TX/RX Switches in 5G Base Stations. Journal of Electronic Materials, (2022) 51:1215–1225.

[15] Y. C. Teng: Improved Synthesis Tool for Miller OTA Stage Using gm/ID Methodology. (2011), Doctoral dissertation, The Ohio State University.

[16] O. Axelsson and K. Andersson.: Highly Linear Gallium Nitride MMIC LNAs. Compound Semiconductor Integrated Circuit Symposium, San Diego, 2012.

[17] Z. Wang, D. Hou, J. Chen, et al.: A Q-Band Self-Biased LNA in 0.1-μm GaAs pHEMT Technology, 2019 12th UK-Europe-China Workshop on Millimeter Waves and Terahertz Technologies (UCMMT), London, 2019: 1-4.

[18] T. Qi, S. He: Design of broadband LNA using improved self-bias architecture, Journal of Circuits, Systems and Computers, 2019, 28(08): 1920005.

[19] Mondal S, Singh R, Hussein A I, et al.: A 25–30 GHz fully-connected hybrid beamforming receiver for MIMO communication. IEEE Journal of Solid-State Circuits, (2018), 53(5): 1275-1287.

[20] Luo J, He J, Wang H, Chang S, Huang Q, Yu X-P. A 28 GHz LNA using defected ground structure for 5G application. Microw Opt Technol Lett. (2018), 60: 1067–1072.

List of figures and tables

Fig. 1. Small-signal circuit model of GaN HEMT at the bias point of V_g=-2 V and V_d=15 V.
Fig. 2. The measured (blue circle) and modelled (red line) *S*-parameters. The frequency range is from 0.2 to 60 GHz.
Fig. 3. Simplified schematic of the designed LNA.
Fig. 4. Photograph of the fabricated LNA.
Fig. 5. Measured S_{11} (a) and S_{22} (b) of different bias points.
Fig. 6. Measured S_{21} (a) and *NF* (b) of different bias points.
Fig. 7. Measured P_{1dB} (a) and *OIP3* (b) of different bias points.
Fig. 8. Measured gain and output power versus input power at 28 GHz (biased at V_d=15 V, with RF and DC pads bonded to board).
Table 1. Extracted intrinsic small-signal parameters of the GaN HEMTs.
Table 2. Comparisons of LNAs for mmWave 5G using different semiconductor technologies.